Received: 5 February 2024 | Revised: 15 March 2024 | Accepted: 20 March 2024

DOI: 10.1111/cts.13788

ARTICLE

Modeling the subcutaneous pharmacokinetics of antibodies co-administered with rHuPH20

Ryan P. Nolan | **Marie A. Printz**

Halozyme Therapeutics, San Diego, California, USA

Correspondence
Ryan P. Nolan, Halozyme Therapeutics, 12390 El Camino Real, San Diego, CA 92130, USA.
Email: rnolan@halozyme.com

Abstract

Predicting the subcutaneous (SC) pharmacokinetics (PK) of antibodies in humans is challenging, with clinical data currently being the only reliable data source for modeling SC absorption and bioavailability. Recombinant human hyaluronidase PH20 (rHuPH20) is an enzyme that facilitates SC delivery of high-dose, high-volume therapeutics. Numerous monoclonal antibodies have been co-administered SC with rHuPH20 in a clinical setting, establishing an extensive PK database. The goal of this work is to demonstrate how aggregated clinical data can be leveraged in a universal modeling framework for characterizing SC antibody PK, resulting in parameterization that can be used in predictive simulations of new antibodies. Data for 10 individual antibodies co-administered SC with rHuPH20 were obtained from publicly available sources. PK modeling of each antibody was conducted using the same model structure, but uniquely parameterized. The model structure consisted of a two-compartment model to capture linear kinetics, plus a target-binding mechanism to accommodate nonlinear kinetics driven by antibody-target complex formation and elimination. The clinical PK profiles for all antibodies were accurately described using the universal modeling framework. The SC PK parameters of absorption and bioavailability were consistent across the range of antibody and target properties evaluated. SC administration with rHuPH20 yielded a 30% increase in absorption rate on average and similar or better bioavailability. These parameter values can serve as initial conditions for model-based PK predictions for new antibodies co-administered SC with rHuPH20 to enable evaluation of optimal SC dose and schedule regimens prior to and during clinical development.

Study highlights

WHAT IS THE CURRENT KNOWLEDGE ON THE TOPIC?

Preclinical animal models are of limited utility for translating/predicting SC PK of antibodies in human. Meta-analysis of clinical SC PK data/parameters across multiple antibodies has been limited to a few antibodies[1]; none of the analyses have evaluated the impact of hyaluronidase.

WHAT QUESTION DID THIS STUDY ADDRESS?

Are the SC-relevant PK parameters of clinical antibodies sufficiently generalizable across various antibody and target systems, and is there a difference when co-administered with rHuPH20?

WHAT DOES THIS STUDY ADD TO OUR KNOWLEDGE?

This study demonstrates that when rHuPH20 is used to facilitate SC administration of antibodies in human, the SC PK parameters of absorption rate and bioavailability are generally consistent. Additionally, a target-engagement kinetic model can potentially serve as a universally applicable framework to accurately model the PK of most antibody-target systems. Finally, this is the first time all clinical antibodies co-administered with rHuPH20 have been collated and comprehensively analyzed.

HOW MIGHT THIS CHANGE CLINICAL PHARMACOLOGY OR TRANSLATIONAL SCIENCE?

This work suggests that aggregated clinical data can sufficiently and reliably be used to establish initial PK model parameterization for a new antibody delivered SC in human, and that investment in the development of animal models for PK translation/prediction may not be needed. The data presented herein can be used as a foundational reference for study design and more refined modeling of SC antibodies, particularly those administered with hyaluronidase.

INTRODUCTION

The number of antibodies approved for SC delivery has increased in recent years.[2,3] The increase in SC adoption can be attributed to its numerous potential benefits over IV administration. For the healthcare system, these include simplified administration, lower costs, reduced provider time, and potentially increased patient throughput associated with shorter patient chair time. For patients, it can reduce the treatment burden and improve quality of life via reduced administration time, and it may allow for self- or caregiver administration in a setting other than an infusion center, for example, home or local doctor's office.[4,5] Also, SC administration may confer PK/PD benefits compared to IV; the flatter PK profile can be advantageous for reducing C_{max}-driven toxicities and/or improving C_{min}-driven efficacy.

In this light, characterization of the SC PK profile of new antibodies is often desirable before clinical development to evaluate various dosing regimens. However, predicting SC PK of antibodies in human from preclinical data is challenging, as there are significant differences in the SC absorption rate and bioavailability across species, none of which reproducibly correlate with what is observed in humans.[6,7] This lack of fundamental and mechanistic understanding of SC absorption has been broadly recognized by the industry as a necessary problem to solve to enable more efficient clinical development of SC therapies.[2]

Such limitations extend to modeling SC PK. Modeling the IV PK of antibodies is straightforward, with well-established frameworks for capturing linear and nonlinear PK profiles.[8] While expressions for SC absorption and bioavailability can be incorporated into these modeling frameworks, the utility is limited to a posteriori characterization rather than a priori prediction.

ENHANZE® drug delivery technology is based on the proprietary recombinant human hyaluronidase PH20 enzyme (rHuPH20; Halozyme Therapeutics, Inc.) that facilitates the SC delivery of co-administered therapeutics. rHuPH20 degrades the glycosaminoglycan hyaluronan, which plays a role in resistance to bulk fluid flow in the SC space, limiting large-volume SC drug delivery, dispersion, and absorption. Co-administration with rHuPH20 can overcome administration time and volume barriers associated with SC formulations, especially for high-dose, high-volume therapeutics.[9]

rHuPH20 is approved in several commercial SC products, five of which are monoclonal antibodies: daratumumab (Darzalex FASPRO®/DARZALEX® SC), trastuzumab (Herceptin Hylecta™/Herceptin® SC), pertuzumab/trastuzumab (Phesgo®), and rituximab (Rituxan Hycela®/MabThera®) in the United States, and atezolizumab (Tecentriq® SC) in Great Britain. SC PK data from these programs, as well as several other antibodies in clinical development with rHuPH20, were leveraged in this work.[10–18] Other drug modalities commercialized with rHuPH20, that is, polyclonal IgG

(HyQvia®) and efgartigimod alfa (antibody fragment) (VYVGART® HYTRULO), were not included in the analysis.

The objective of this work is to characterize the human SC PK of antibodies, specifically when co-administered with rHuPH20. Specifically, we demonstrate how an aggregated set of clinical data for various antibodies can be leveraged in a straightforward, universal framework for modeling SC antibody PK. The parameterization from such an approach can provide a reliable starting point for predicting the human SC PK of new antibodies and enable more streamlined clinical development of such therapies.

METHODS

Data collection

The data used in this analysis consisted of 10 monoclonal antibodies that were co-administered SC with rHuPH20 in human clinical studies. All 10 antibodies have data from IV administration and SC administration with rHuPH20, and five antibodies additionally have data from SC administration without rHuPH20. All data are publicly available and are referenced in Table 1 and depicted in Figure 2.

Model definition

PK models have been previously developed and published for most of the antibodies in this analysis (see data references in Table 1). These models leveraged a two-compartment model structure for linear PK, and, when appropriate, accounted for nonlinear kinetics by introducing saturable clearance expressions, for example, Michaelis-Menten, to the central compartment. While the same linear compartmental structure was used in this analysis, the nonlinear approach was replaced with a more mechanistic, streamlined format.[19] Specifically, PK nonlinearity, often characterized as target-mediated drug disposition, was accounted for via incorporation of antibody-target binding kinetics and an antibody-target complex elimination pathway; such an approach allows for the antibody affinity (i.e., equilibrium binding constant, K_d), intrinsic target (steady-state) concentration, and target kinetics (i.e., target half-life) to drive the total (free and bound) antibody PK with one universally applicable framework. If the target is not expressed at significant levels or its turnover is of long enough duration, its impact on the antibody PK will be negligible, with the kinetics following that of a two-compartment model. If the target is highly expressed and/or has a short half-life, this will introduce an additional saturable, nonlinear clearance pathway for the antibody that provides a similar kinetic influence as introducing a Michaelis-Menten expression. The additional benefit of leveraging such a target-binding mechanism is that the associated parameters can be defined a priori based on literature data, as described below. A schematic of the model structure, differential equations, and description of the parameters are in Figure 1.

Initial parameter estimates

Initial estimates for the two-compartment parameters, that is, V_1 and V_2 (volumes of the central (plasma) and peripheral (tissue interstitial) compartments, respectively), k_{el} (central compartment elimination rate), k_{12} and k_{21} (distribution rates for central→peripheral and peripheral→central compartments, respectively), and F (bioavailability for SC administration without rHuPH20), were defined from the previously published PK models for each of the respective antibodies. For antibodies where published data were not available, generalized population PK parameters derived from Dirks et al.[20] were used.

For target and antibody-target kinetic parameters, that is, T_{ss} (target steady-state concentration), k_{syn} and k_{deg} (target synthesis and degradation rates, respectively), k_{on} and k_{off} (antibody association and dissociation rates, respectively), and k_{deg2} (antibody-target complex degradation/elimination rate), data from published literature were used. Once defined, these parameters were fixed and not considered for subsequent optimization.

Since two types of targets exist, soluble or cell-surface, slight differences in the parameterization were considered for each. For soluble targets, steady-state concentrations were readily measurable, and clearance for the antibody-target complex was assumed to follow that of the antibody, that is, $k_{deg2} = k_{el}$. For cell-surface targets, steady-state concentrations (in units of nM) were derived from receptor (target) density (X_R, in units of receptors/cell) and cell density (X_C, in units of cells/L) according to: $T_{ss} = X_R \cdot X_C / N_A \cdot 10^9$, where N_A is Avogadro's Number (i.e., 6.02e23), and clearance for the antibody-target complex was assumed to follow that of the target, that is, $k_{deg2} = k_{deg}$. Once defined, target concentrations were fixed and not considered for subsequent optimization. All data sources and derivations are described in Table 1.

Parameter fitting

For each antibody, parameter fitting was conducted for the collective datasets (i.e., all dose levels and routes of administration) as a Population PK (PopPK) assessment.

TABLE 1 Data sources, parameter values, and derivations for each antibody.

Parameter	Description	Units	Trastuzumab	Daratumumab	Rituximab
—	Target	—	HER2	CD38	CD20
—	Target Location	—	Cell	Cell	Cell
—	IV PK Data	—	[16]	[24]	[16,25]
—	SC PK Data with rHuPH20	—	[16]	[17]	[16]
—	SC PK Data without rHuPH20	—	—	—	—
V_1	Central Volume	L	2.20 [F]	3.10 [20]	2.50 [F]
V_2	Peripheral Volume	L	3.06 [34]	2.80 [20]	3.64 [35]
CL	Central Clearance	L/day	0.11 [34]	0.31 [20]	0.10 [F]
Q	Distributional Clearance	L/day	0.45 [34]	0.79 [20]	0.66 [35]
k_{el}	Central Elimination Rate	1/day	0.05 [C]	0.10 [C]	0.04 [C]
k_{12}	Central-Peripheral Rate	1/day	0.20 [C]	0.25 [C]	0.26 [C]
k_{21}	Peripheral-Central Rate	1/day	0.15 [C]	0.28 [C]	0.18 [C]
k_a	SC Absorption Rate	1/day	—	—	—
k_{aPH20}	SC Absorption Rate with PH20	1/day	0.40 [34]	0.28 [38]	0.37 [39]
F	SC Bioavailability	Fraction	—	—	—
F_{PH20}	SC with PH20 Bioavailability	Fraction	0.77 [34]	0.69 [38]	0.63 [39]
T_{ss}	Target Concentration	nM	7.58 [C]	0.17 [C]	1.67 [C]
t_{half}	Target Half-Life	day	0.42 [44]	0.13 [45]	0.17 [46]
K_d	Antibody Affinity	nM	5.00 [52]	4.40 [53]	8.00 [54]
k_{syn}	Target Synthesis Rate	nM/day	12.5 [C]	0.89 [C]	6.80 [C]
k_{deg}	Target Degradation Rate	1/day	1.65 [C]	5.33 [C]	4.08 [C]
k_{on}	Antibody-Target On Rate	1/nM·day	86.4[c]	86.4[c]	86.4[c]
k_{off}	Antibody-Target Off Rate	1/day	432 [C]	380 [C]	691 [C]
k_{deg2}	Antibody-Target Degradation Rate	1/day	1.65 [C]	5.33 [C]	4.08 [C]
X_R	Receptor Density	Receptors/cell	1.00e6 [61]	1.00e5 [62]	1.00e5 [63]
X_C	Cell Density	Cells/L	4.55e9 [65]	1.00e9[d]	1.00e10 [66]

Abbreviations: —, not applicable/available; [C], calculated, according to the following: k_{el}, CL/V_1; k_{12}, Q/V_1; k_{21}, Q/V_2; $T_{ss} = X_R \cdot X_C / N_A \cdot 10^9$; k_{syn}, $T \cdot k_{deg}$; k_{deg}, $\ln(2)/t_{½}$; k_{off}, $K_d \cdot k_{on}$; k_{deg2}, k_{deg} (cell target) or k_{el} (soluble target); [F] = fit from data; a, treated as one target; b, treated as soluble; c, assumed diffusion-limited rate of 10^6 1/M·s; d, assumed value.

Covariates were not incorporated, as the average representation of the respective population is sufficient for this application. Initial simulations were conducted using the initial parameter estimates for the respective antibody and target to assess goodness of fit across the collective datasets, that is, all concentration versus time profiles. The default preference was to keep the previously defined, published parameters (i.e., clearances and volumes) unchanged, but for some antibodies re-fitting was necessary. If the simulated curves deviated from the observed data by more than 10% for a given timepoint, then parameter optimization was conducted on the necessary parameters only. For example, if the initial parameters accurately captured the IV curves but not the SC curves, then only the SC relevant parameters (e.g., F and k_{abs}) were re-defined using a least-sum-of-squares optimization routine. In Table 1, the source of each parameter for each antibody is specified. All simulations were performed using MATLAB® (Mathworks, Natick, MA).

RESULTS

Model fitting

Figure 2 shows the ability of the model-simulated PK profiles to reproduce the measured clinical data for each antibody and route of administration. Model parameterization of IV data derived from previously published models proved an appropriate starting point for most antibodies, with no further modification to these two-compartment parameters (i.e., V_1, V_2, CL, Q, k_a, F) upon introduction of SC data with rHuPH20. For some antibodies, the new data did require slight changes to one or more of these parameters to enable cohesive fitting of curves from all routes

Atezolizumab	Pertuzumab	Crenezumab	Tocilizumab	Bococizumab	Adalimumab	Amivantamab
PD-L1	HER2	Aβ40	(s)IL6R	PCSK9	TNFα	EGFR-MET [a]
Soluble	Cell	Soluble	Cell, Soluble [b]	Soluble	Soluble	Cell
[26]	[18]	[27]	[28]	[29]	[30]	[31]
[13]	[18]	[11]	[15]	[10]	[12]	[14]
—	—	[11]	[15,28]	[10]	[12,32]	[14]
3.28 [26]	2.77 [18]	2.90 [11]	3.50 [F]	2.75 [33]	3.10 [20]	2.00 [F]
3.63 [26]	2.49 [18]	1.60 [11]	2.80 [20]	3.02 [33]	2.80 [20]	2.80 [20]
0.20 [26]	0.16 [18]	0.18 [11]	0.40 [F]	0.30 [F]	0.31 [20]	0.20 [F]
0.55 [26]	0.62 [18]	0.15 [11]	0.79 [20]	0.28 [33]	0.79 [20]	0.79 [20]
0.06 [C]	0.06 [C]	0.06 [C]	0.11 [C]	0.11 [C]	0.10 [C]	0.10 [C]
0.17 [C]	0.22 [C]	0.05 [C]	0.23 [C]	0.10 [C]	0.25 [C]	0.40 [C]
0.15 [C]	0.25 [C]	0.09 [C]	0.28 [C]	0.09 [C]	0.28 [C]	0.28 [C]
—	—	0.35 [F]	0.23 [36]	0.25 [33]	0.26 [37]	0.25 [F]
0.27 [13]	0.35 [18]	0.35 [F]	0.40 [F]	0.40 [F]	0.30 [F]	0.40 [F]
—	—	0.80 [F]	0.80 [36]	0.30 [F]	0.70 [F]	0.62 [F]
0.77 [13]	0.71 [18]	0.80 [F]	0.90 [F]	0.33 [F]	0.85 [F]	0.82 [F]
0.002 [40]	6.02 [C]	0.06 [C]	0.87 [41]	6.76 [42]	0.0003 [43]	0.83 [C]
0.67 [47]	0.42 [44]	0.13 [48]	0.08 [49]	0.10 [33]	0.02 [50]	0.17 [51]
0.30 [55]	0.80 [56]	4.00 [57]	1.34 [58]	0.01 [33]	0.10 [59]	0.70 [60]
0.00 [C]	9.93 [C]	0.35 [C]	7.20 [C]	46.9 [C]	0.01 [C]	3.47 [C]
1.04 [C]	1.65 [C]	5.55 [C]	8.32 [C]	6.93 [C]	33.3 [C]	4.16 [C]
86.4[c]	86.4[c]	86.4[c]	86.4[c]	86.4[c]	86.4[c]	86.4[c]
25.9 [C]	69.1 [C]	346 [C]	116 [C]	0.86 [C]	8.64 [C]	60.5 [C]
0.06 [C]	1.65 [C]	0.06 [C]	8.32 [C]	0.11 [C]	0.10 [C]	4.16 [C]
—	1.00e6 [61]	—	—	—	—	5.00e5 [64]
—	3.61e9 [65]	—	—	—	—	1.00e9 [67,68]

of administration (see Table 1). The results highlight that the universal, pre-defined framework presented herein can capture linear and nonlinear kinetics across various antibodies and targets. Furthermore, the extent of target-mediated drug disposition can be defined a priori, that is, independent of the PK data, based on target expression and half-life, and antibody affinity and dose.

Parameter values

Figure 3 and Table 1 outline the specific parameter values for each antibody. The volumes of distribution (V_1, V_2) demonstrate high degrees of consistency across antibodies (~20% coefficient of variation (CV)), while central and distributional clearances (CL, Q) have higher degrees of variability across antibodies (~40% CV). Absorption rates without and with rHuPH20 are highly consistent across antibodies (<20% CV). The absorption rate with rHuPH20 is approximately 30% higher than without, which is congruent with the mechanism of rHuPH20, wherein its degradation of hyaluronan reduces the SC tissue back-pressure and accommodates larger volumes at the injection site.[9] Bioavailability without and with rHuPH20 is consistent across antibodies (~12% CV), except for the one outlier which was not included in the average calculations. Bioavailability with rHuPH20 demonstrated improvements ranging from 0% to 20% (absolute, i.e., bioavailability % as it relates to IV) relative to values without rHuPH20, for the five antibodies for which data were available for both administrations.

A large range was observed across parameters related to target engagement. Target concentrations ranged from sub-pM to nM, target half-lives ranged from minutes to several hours, and antibody affinities ranged from tens of pM to nM.

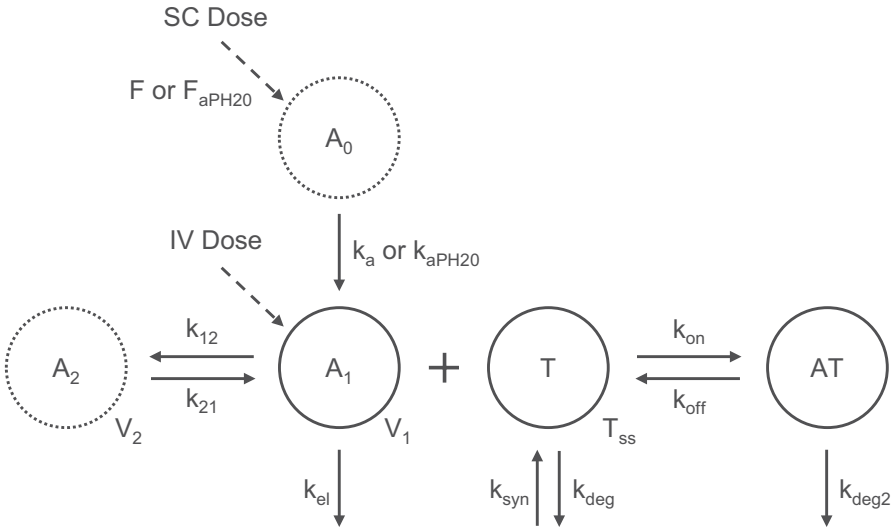

$$dA_0/dt = -k_{abs}\cdot A_0$$

$$dA_1/dt = k_{abs}\cdot A_0/V_1 - k_{12}\cdot A_1 + k_{21}\cdot A_2\cdot(V_2/V_1) - k_{el}\cdot A_1 - k_{on}\cdot A_1\cdot T + k_{off}\cdot AT$$

$$dA_2/dt = k_{12}\cdot A_1\cdot(V_1/V_2) - k_{21}\cdot A_2$$

$$dT/dt = -k_{on}\cdot A_1\cdot T + k_{off}\cdot AT + k_{syn} - k_{deg}\cdot T$$

$$dAT/dt = k_{on}\cdot A_1\cdot T - k_{off}\cdot AT - k_{deg2}\cdot AT$$

FIGURE 1 PK model schematic and differential equations. Model variables: A_0, A_1, and A_2 = antibody in the subcutaneous, central (plasma), and peripheral (tissue interstitial) compartments, respectively; T = target; AT = antibody-target complex. Model parameters: V_1 and V_2 = volumes of the central and peripheral compartments, respectively; k_{el} = central compartment elimination rate; k_{12} and k_{21} = distribution rates for central→peripheral and peripheral→central compartments, respectively; k_a and k_{aPH20} = absorption rates for subcutaneous→central compartments, without and with rHuPH20, respectively; F and F_{PH20} = subcutaneous bioavailability, without and with rHuPH20, respectively; T_{ss} = target steady-state concentration; k_{syn} and k_{deg} = target synthesis and degradation rates, respectively; k_{on} and k_{off} = antibody association and dissociation rates, respectively. k_{deg2} = antibody-target complex degradation/elimination rate. Further details, including derivations and units, are in Table 1.

DISCUSSION

Preclinical data have been of limited utility in predicting SC PK of antibodies in human to date. In this work, a different approach was taken by focusing on a universally applicable model to characterize the human PK profiles of 10 clinical antibodies co-administered SC with rHuPH20. The linear PK aspects driven by two-compartment model kinetics were consistent across antibodies in this analysis and aligned with previous works.[20,21] The nonlinear PK contributions were captured via a mechanistic target engagement framework and a priori-defined values for target and antibody parameters. For antibodies co-administered with rHuPH20, the human SC PK parameters are quite consistent across a range of antibody and target properties. Consequently, the average values in this work can be applied with a high degree of confidence in model simulations for a new antibody prior to entering the clinic to evaluate potential dosing and schedule options for SC co-administration with rHuPH20.

The SC PK parameterization can be leveraged via a few angles in Phase I as well. If an adaptive design is used, the parameter values can serve as priors. Additionally, when considering the ability of rHuPH20 to accommodate any dose level or volume, Phase I dose escalation could occur exclusively SC, that is, without IV data. As an example, HyQvia®, a commercial product comprised polyclonal IgG and rHuPH20, is dosed up to 600 mL in a single SC infusion[22]; when considering dose escalation of an antibody up to 100 mg/kg, even with a modest formulation of 100 mg/mL, such a volume would be less than 100 mL and easily accommodated. Starting SC clinical trials with a low-concentration, high-volume formulation with rHuPH20 is also an option. Such a path was taken by Darzalex FASPRO®, wherein the initial SC Phase I studies utilized a 20 mg/mL formulation administered at volumes

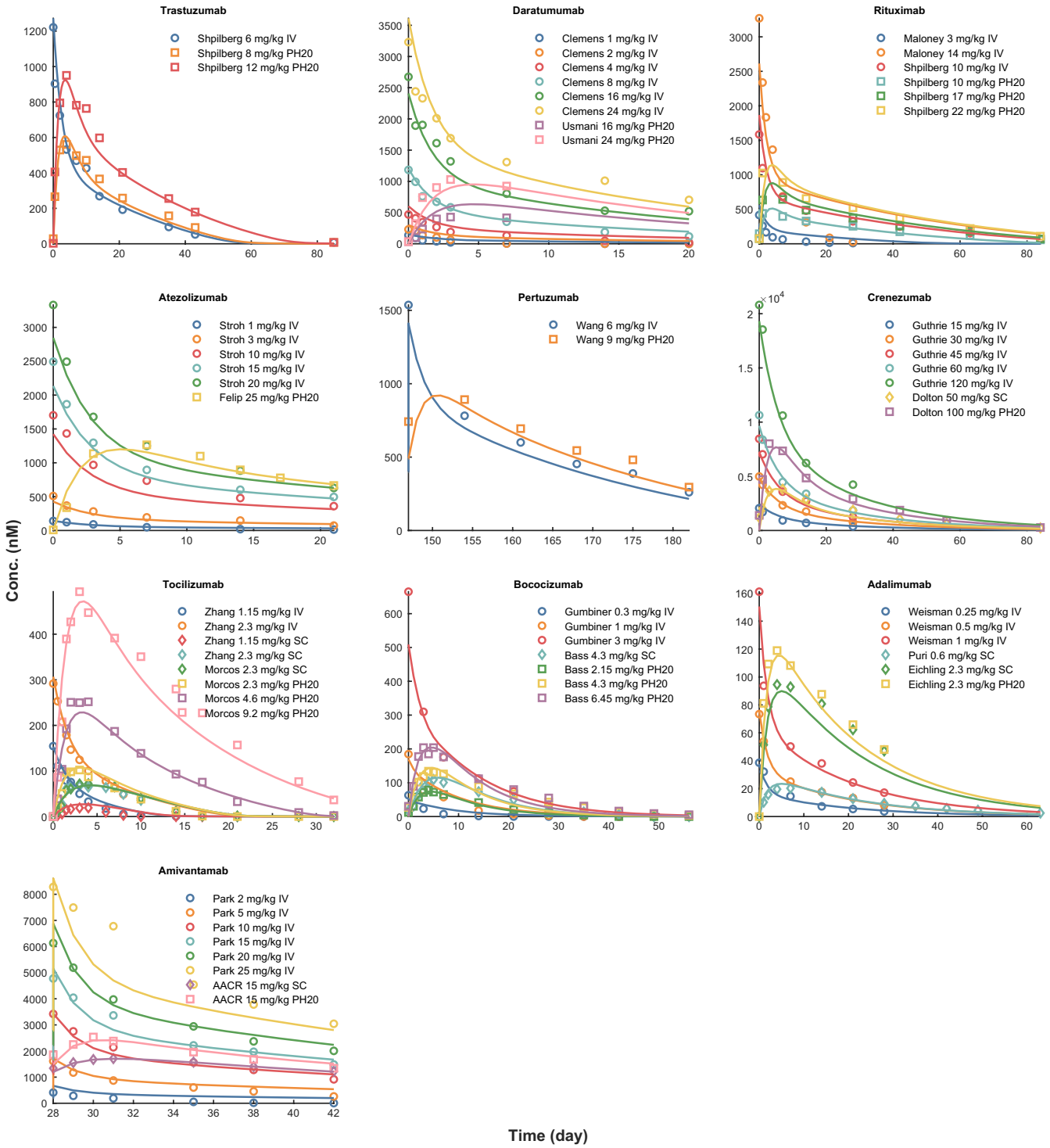

FIGURE 2 Model simulated PK profiles versus measured clinical data. Symbols represent measured mean clinical data, digitized from the respective publications; curves represent model simulations. Routes of administration are distinguished based on the following symbol shapes: ○ = intravenous (IV); ◇ = subcutaneous without rHuPH20 (SC); □ = subcutaneous with rHuPH20 (PH20).

up to 90 mL with rHuPH20.[17] While there has been a precedent to date for IV studies preceding SC, this is not an explicit requirement. In fact, for oral drug delivery, IV PK studies are not always required in humans and for many molecules are never executed.[23] Based on the analysis presented herein, and the new PK data that continues to be generated for antibodies co-administered with rHuPH20, such an analogous SC clinical development path is now possible.

Despite the high degree of consistency in the PK parameters across antibodies, and the ability to capture/predict PK nonlinearities, there will inevitably be instances where

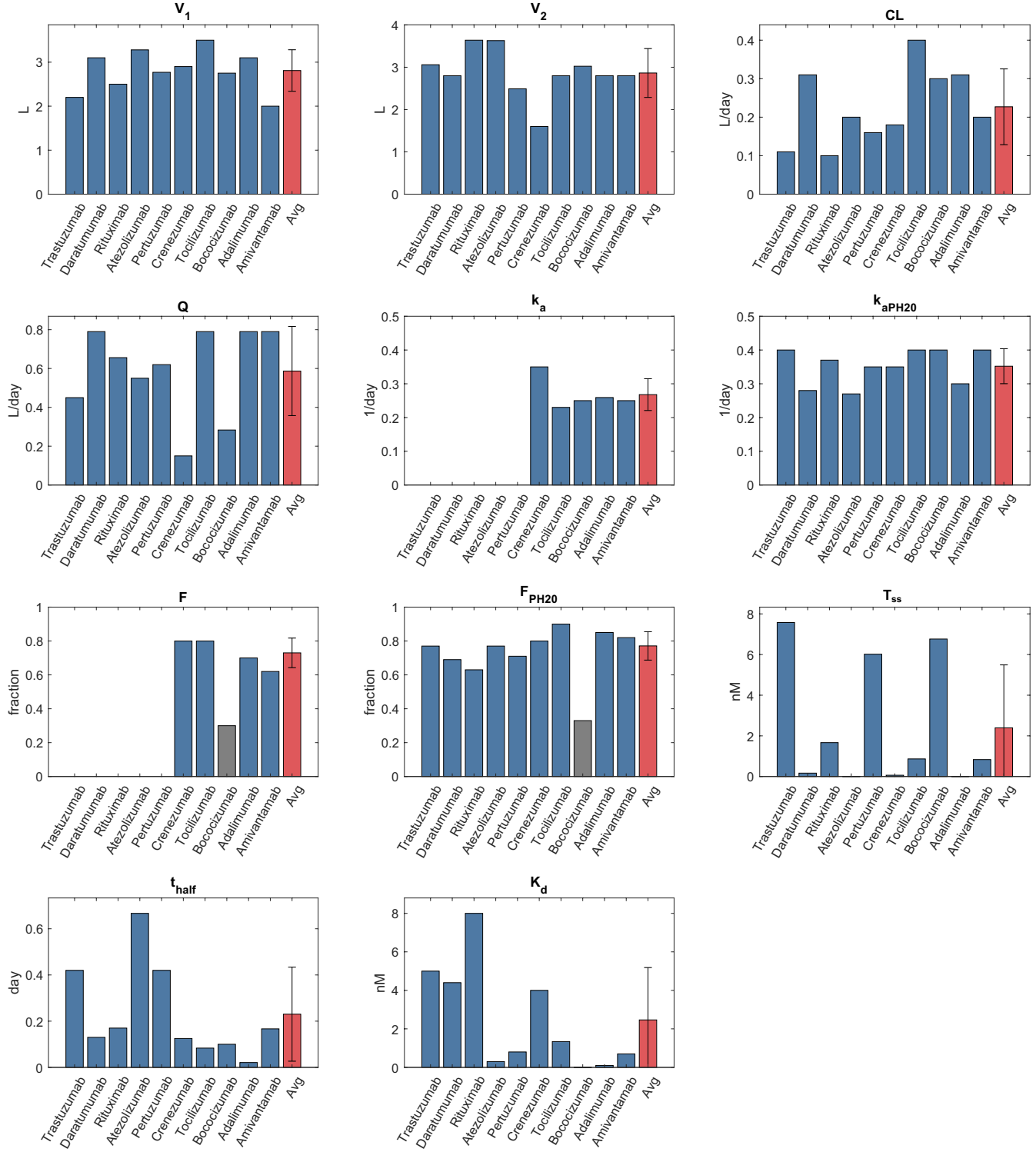

FIGURE 3 Model parameters. Parameter values are listed for the population fit of data for each respective antibody. Red bars designate the average across all antibodies shown, with error bars representing standard deviation. Bococizumab was excluded from the calculation of the average values for F and F_{PH20}, as it was a significant outlier across the antibodies for these specific parameters.

this methodology does not accurately predict the SC PK, specifically bioavailability, as was observed with the one outlier in this analysis. Therefore, there will continue to be a need to establish correlations with the variables involved in SC absorption and clinical PK. With more antibodies being delivered SC and the broad adoption of data analytics and artificial intelligence, the probability of accurately predicting bioavailability anomalies will increase over time.

AUTHOR CONTRIBUTIONS

R.P.N. wrote the manuscript. R.P.N. analyzed the data. R.P.N. performed the modeling. R.P.N. and M.A.P. designed the research.

ACKNOWLEDGMENTS

The authors would like to thank Stephen Knowles and Michael LaBarre (Halozyme Therapeutics, Inc., San Diego, CA, USA) for their scientific guidance in the development of this work.

FUNDING INFORMATION

This work was supported by Halozyme Therapeutics, Inc.

CONFLICT OF INTEREST STATEMENT

R.P.N. and M.A.P. are employees of Halozyme Therapeutics, Inc. R.P.N. and M.A.P. are shareholders of Halozyme Therapeutics, Inc.

REFERENCES

1. Davda JP, Dodds MG, Gibbs MA, Wisdom W, Gibbs JP. A model-based meta-analysis of monoclonal antibody pharmacokinetics to guide optimal first-in-human study design. *MAbs*. 2014;6(4):1094-1102.
2. Sanchez-Felix M, Burke M, Chen HH, Patterson C, Mittal S. Predicting bioavailability of monoclonal antibodies after subcutaneous administration: open innovation challenge. *Adv Drug Deliv Rev*. 2020;167:66-77.
3. Viola M, Sequeira J, Seiça R, et al. Subcutaneous delivery of monoclonal antibodies: how do we get there? *J Control Release*. 2018;286:301-314.
4. Bittner B, Richter W, Schmidt J. Subcutaneous administration of biotherapeutics: an overview of current challenges and opportunities. *BioDrugs*. 2018;32(5):425-440.
5. De Cock E, Pivot X, Hauser N, et al. A time and motion study of subcutaneous versus intravenous trastuzumab in patients with HER2-positive early breast cancer. *Cancer Med*. 2016;5(3):389-397.
6. Richter WF, Bhansali SG, Morris ME. Mechanistic determinants of biotherapeutics absorption following SC administration. *AAPS J*. 2012;14(3):559-570.
7. Richter WF, Jacobsen B. Subcutaneous absorption of biotherapeutics: knowns and unknowns. *Drug Metab Dispos*. 2014;42(11):1881-1889.
8. Pasquiers B, Benamara S, Felices M, Nguyen L, Declèves X. Review of the existing translational pharmacokinetics modeling approaches specific to monoclonal antibodies (mAbs) to support the first-in-human (FIH) dose selection. *Int J Mol Sci*. 2022;23(21):12754.
9. Locke KW, Maneval DC, LaBarre MJ. ENHANZE((R)) drug delivery technology: a novel approach to subcutaneous administration using recombinant human hyaluronidase PH20. *Drug Deliv*. 2019;26(1):98-106.
10. Bass A, Plotka A, Mridha K, Sattler C, Kim AM, Plowchalk DR. Pharmacokinetics, pharmacodynamics, and safety of bococizumab, a monoclonal antibody against proprotein convertase subtilisin/kexin type 9, in healthy subjects when administered in co-mixture with recombinant human hyaluronidase: a phase 1 randomized trial. *Health Sci Rep*. 2018;1(9):e61.
11. Dolton MJ, Chesterman A, Moein A, et al. Safety, tolerability, and pharmacokinetics of high-volume subcutaneous crenezumab, with and without recombinant human hyaluronidase in healthy volunteers. *Clin Pharmacol Ther*. 2021;110(5):1337-1348.
12. Eichling S. Establishing in vitro, ex vivo and in vivo models to study the behavior of monoclonal antibody formulations upon subcutaneous injection. 2018. Natural Sciences and Mathematics, Ruperto-Carola University of Heidelberg, Germany.
13. Felip E, Burotto M, Zvirbule Z, et al. Results of a dose-finding phase 1b study of subcutaneous Atezolizumab in patients with locally advanced or metastatic non-small cell lung cancer. *Clin Pharmacol Drug Dev*. 2021;10(10):1142-1155.
14. Krebs MG. *Subcutaneous Delivery of Amivantamab in Patients with Advanced Solid Malignancies: Initial Safety and Pharmacokinetic Results from the PALOMA Study*. American Association for Cancer Research; 2022.
15. Morcos PN, Zhang X, McIntyre C, Bittner B, Rowell L, Hussain Z. Pharmacokinetics and pharmacodynamics of single subcutaneous doses of tocilizumab administered with or without rHuPH20. *Int J Clin Pharmacol Ther*. 2013;51(7):537-548.
16. Shpilberg O, Jackisch C. Subcutaneous administration of rituximab (MabThera) and trastuzumab (Herceptin) using hyaluronidase. *Br J Cancer*. 2013;109(6):1556-1561.
17. Usmani SZ, Nahi H, Mateos MV, et al. Subcutaneous delivery of daratumumab in relapsed or refractory multiple myeloma. *Blood*. 2019;134(8):668-677.
18. Wang B, Deng R, Hennig S, et al. Population pharmacokinetic and exploratory exposure-response analysis of the fixed-dose combination of pertuzumab and trastuzumab for subcutaneous injection in patients with HER2-positive early breast cancer in the FeDeriCa study. *Cancer Chemother Pharmacol*. 2021;88(3):499-512.
19. Spilker ME, Singh P, Vicini P. Mathematical modeling of receptor occupancy data: a valuable technology for biotherapeutic drug development. *Cytometry B Clin Cytom*. 2016;90(2):230-236.
20. Dirks NL, Meibohm B. Population pharmacokinetics of therapeutic monoclonal antibodies. *Clin Pharmacokinet*. 2010;49(10):633-659.
21. Betts A, Keunecke A, van Steeg TJ, et al. Linear pharmacokinetic parameters for monoclonal antibodies are similar within a species and across different pharmacological targets: a comparison between human, cynomolgus monkey and hFcRn Tg32 transgenic mouse using a population-modeling approach. *MAbs*. 2018;10(5):751-764.
22. Takeda. HYQVIA [Immune Globulin Infusion 10% (Human) with Recombinant Human Hyaluronidase]. FDA label 2014. https://www.fda.gov/media/89844/download
23. Ohtani H, Iwata R, Imaoka A, Akiyoshi T. Estimation of absolute oral bioavailability without performing an intravenous clinical study. *Drug Metab Pharmacokinet*. 2021;38:100392.
24. Clemens PL, Yan X, Lokhorst HM, et al. Pharmacokinetics of daratumumab following intravenous infusion in relapsed or refractory multiple myeloma after prior proteasome inhibitor and immunomodulatory drug treatment. *Clin Pharmacokinet*. 2017;56(8):915-924.

25. Maloney DG, Liles TM, Czerwinski DK, et al. Phase I clinical trial using escalating single-dose infusion of chimeric anti-CD20 monoclonal antibody (IDEC-C2B8) in patients with recurrent B-cell lymphoma. *Blood*. 1994;84(8):2457-2466.
26. Stroh M, Winter H, Marchand M, et al. Clinical pharmacokinetics and pharmacodynamics of Atezolizumab in metastatic urothelial carcinoma. *Clin Pharmacol Ther*. 2017;102(2):305-312.
27. Guthrie H, Honig LS, Lin H, et al. Safety, tolerability, and pharmacokinetics of crenezumab in patients with mild-to-moderate Alzheimer's disease treated with escalating doses for up to 133 weeks. *J Alzheimers Dis*. 2020;76(3):967-979.
28. Zhang X, Georgy A, Rowell L. Pharmacokinetics and pharmacodynamics of tocilizumab, a humanized anti-interleukin-6 receptor monoclonal antibody, following single-dose administration by subcutaneous and intravenous routes to healthy subjects. *Int J Clin Pharmacol Ther*. 2013;51(6):443-455.
29. Gumbiner B, Joh T, Liang H, et al. The effects of single- and multiple-dose administration of bococizumab (RN316/PF-04950615), a humanized IgG2Deltaa monoclonal antibody binding proprotein convertase subtilisin/kexin type 9, in hypercholesterolemic subjects treated with and without atorvastatin: results from four phase I studies. *Cardiovasc Ther*. 2018;36(1):1-12.
30. Weisman MH, Moreland LW, Furst DE, et al. Efficacy, pharmacokinetic, and safety assessment of adalimumab, a fully human anti-tumor necrosis factor-alpha monoclonal antibody, in adults with rheumatoid arthritis receiving concomitant methotrexate: a pilot study. *Clin Ther*. 2003;25(6):1700-1721.
31. Park K, Haura EB, Leighl NB, et al. Amivantamab in EGFR exon 20 insertion-mutated non-small-cell lung cancer progressing on platinum chemotherapy: initial results from the CHRYSALIS phase I study. *J Clin Oncol*. 2021;39(30):3391-3402.
32. Puri A, Niewiarowski A, Arai Y, et al. Pharmacokinetics, safety, tolerability and immunogenicity of FKB327, a new biosimilar medicine of adalimumab/Humira, in healthy subjects. *Br J Clin Pharmacol*. 2017;83(7):1405-1415.
33. Udata C, Garzone PD, Gumbiner B, et al. A mechanism-based pharmacokinetic/pharmacodynamic model for Bococizumab, a humanized monoclonal antibody against proprotein convertase subtilisin/Kexin type 9, and its application in early clinical development. *J Clin Pharmacol*. 2017;57(7):855-864.
34. Quartino AL, Hillenbach C, Li J, et al. Population pharmacokinetic and exposure-response analysis for trastuzumab administered using a subcutaneous "manual syringe" injection or intravenously in women with HER2-positive early breast cancer. *Cancer Chemother Pharmacol*. 2016;77(1):77-88.
35. Ng CM, Bruno R, Combs D, Davies B. Population pharmacokinetics of rituximab (anti-CD20 monoclonal antibody) in rheumatoid arthritis patients during a phase II clinical trial. *J Clin Pharmacol*. 2005;45(7):792-801.
36. Abdallah H, Hsu JC, Lu P, et al. Pharmacokinetic and pharmacodynamic analysis of subcutaneous tocilizumab in patients with rheumatoid arthritis from 2 randomized, controlled trials: SUMMACTA and BREVACTA. *J Clin Pharmacol*. 2017;57(4):459-468.
37. Ternant D, Ducourau E, Fuzibet P, et al. Pharmacokinetics and concentration-effect relationship of adalimumab in rheumatoid arthritis. *Br J Clin Pharmacol*. 2015;79(2):286-297.
38. Luo MM, Usmani SZ, Mateos MV, et al. Exposure-response and population pharmacokinetic analyses of a novel subcutaneous formulation of daratumumab administered to multiple myeloma patients. *J Clin Pharmacol*. 2021;61(5):614-627.
39. Gibiansky E, Gibiansky L, Chavanne C, Frey N, Jamois C. Population pharmacokinetic and exposure-response analyses of intravenous and subcutaneous rituximab in patients with chronic lymphocytic leukemia. *CPT Pharmacometrics Syst Pharmacol*. 2021;10(8):914-927.
40. Asanuma K, Nakamura T, Hayashi A, et al. Soluble programmed death-ligand 1 rather than PD-L1 on tumor cells effectively predicts metastasis and prognosis in soft tissue sarcomas. *Sci Rep*. 2020;10(1):9077.
41. Nishimoto N, Terao K, Mima T, Nakahara H, Takagi N, Kakehi T. Mechanisms and pathologic significances in increase in serum interleukin-6 (IL-6) and soluble IL-6 receptor after administration of an anti-IL-6 receptor antibody, tocilizumab, in patients with rheumatoid arthritis and Castleman disease. *Blood*. 2008;112(10):3959-3964.
42. Lakoski SG, Lagace TA, Cohen JC, Horton JD, Hobbs HH. Genetic and metabolic determinants of plasma PCSK9 levels. *J Clin Endocrinol Metab*. 2009;94(7):2537-2543.
43. Thilagar S, Theyagarajan R, Sudhakar U, Suresh S, Saketharaman P, Ahamed N. Comparison of serum tumor necrosis factor-alpha levels in rheumatoid arthritis individuals with and without chronic periodontitis: a biochemical study. *J Indian Soc Periodontol*. 2018;22(2):116-121.
44. Maass KF, Kulkarni C, Betts AM, Wittrup KD. Determination of cellular processing rates for a trastuzumab-Maytansinoid antibody-drug conjugate (ADC) highlights key parameters for ADC design. *AAPS J*. 2016;18(3):635-646.
45. Funaro A, Reiniš M, Trubiani O, Santi S, di Primio R, Malavasi F. CD38 functions are regulated through an internalization step. *J Immunol*. 1998;160(5):2238-2247.
46. Beum PV, Peek EM, Lindorfer MA, et al. Loss of CD20 and bound CD20 antibody from opsonized B cells occurs more rapidly because of trogocytosis mediated by fc receptor-expressing effector cells than direct internalization by the B cells. *J Immunol*. 2011;187(6):3438-3447.
47. Li CW, Lim SO, Xia W, et al. Glycosylation and stabilization of programmed death ligand-1 suppresses T-cell activity. *Nat Commun*. 2016;7:12632.
48. Ovod V, Ramsey KN, Mawuenyega KG, et al. Amyloid beta concentrations and stable isotope labeling kinetics of human plasma specific to central nervous system amyloidosis. *Alzheimers Dement*. 2017;13(8):841-849.
49. Gerhartz C, Dittrich E, Stoyan T, et al. Biosynthesis and half-life of the interleukin-6 receptor and its signal transducer gp130. *Eur J Biochem*. 1994;223(1):265-274.
50. Ma Y, Zhao S, Shen S, et al. A novel recombinant slow-release TNF alpha-derived peptide effectively inhibits tumor growth and angiogensis. *Sci Rep*. 2015;5:13595.
51. Yu JJ, Zhou DD, Yang XX, et al. TRIB3-EGFR interaction promotes lung cancer progression and defines a therapeutic target. *Nat Commun*. 2020;11(1):3660.

52. Genentech. HERCEPTIN (trastuzumab) FDA label. 1998. https://www.accessdata.fda.gov/drugsatfda_docs/label/1998/trasgen092598lb.pdf
53. van de Donk NW, Janmaat ML, Mutis T, et al. Monoclonal antibodies targeting CD38 in hematological malignancies and beyond. *Immunol Rev*. 2016;270(1):95-112.
54. Genentech. RITUXAN (rituximab) FDA label. 1997. https://www.accessdata.fda.gov/drugsatfda_docs/label/2010/103705s5311lbl.pdf
55. Roche. Tecentriq (atezolizumab) EMA assessment report. 2018. https://www.ema.europa.eu/en/documents/assessment-report/tecentriq-epar-public-assessment-report_en.pdf
56. Roche. Perjeta (Pertuzumab) EMA asssessment report. 2013. https://www.ema.europa.eu/en/documents/assessment-report/perjeta-epar-public-assessment-report_en.pdf
57. Ultsch M, Li B, Maurer T, et al. Structure of crenezumab complex with Abeta shows loss of beta-hairpin. *Sci Rep*. 2016;6:39374.
58. Xu C, Rafique A, Potocky T, et al. Differential binding of sarilumab and tocilizumab to IL-6Ralpha and effects of receptor occupancy on clinical parameters. *J Clin Pharmacol*. 2021;61(5):714-724.
59. Hu S, Liang S, Guo H, et al. Comparison of the inhibition mechanisms of adalimumab and infliximab in treating tumor necrosis factor alpha-associated diseases from a molecular view. *J Biol Chem*. 2013;288(38):27059-27067.
60. Brazel D, Nagasaka M. Spotlight on Amivantamab (JNJ-61186372) for EGFR exon 20 insertions positive non-small cell lung cancer. *Lung Cancer (Auckl)*. 2021;12:133-138.
61. Hicks DG, Kulkarni S. HER2+ breast cancer: review of biologic relevance and optimal use of diagnostic tools. *Am J Clin Pathol*. 2008;129(2):263-273.
62. Kang L, Jiang D, England CG, et al. ImmunoPET imaging of CD38 in murine lymphoma models using (89)Zr-labeled daratumumab. *Eur J Nucl Med Mol Imaging*. 2018;45(8):1372-1381.
63. Horna P, Moscinski LC, Sokol L, Shao H. Naive/memory T-cell phenotypes in leukemic cutaneous T-cell lymphoma: putative cell of origin overlaps disease classification. *Cytometry B Clin Cytom*. 2019;96(3):234-241.
64. Zhang F, Wang S, Yin L, et al. Quantification of epidermal growth factor receptor expression level and binding kinetics on cell surfaces by surface plasmon resonance imaging. *Anal Chem*. 2015;87(19):9960-9965.
65. Lagendijk M, Vos EL, Ramlakhan KP, et al. Breast and tumour volume measurements in breast cancer patients using 3-D automated breast volume scanner images. *World J Surg*. 2018;42(7):2087-2093.
66. Winkler U, Jensen M, Manzke O, Schulz H, Diehl V, Engert A. Cytokine-release syndrome in patients with B-cell chronic lymphocytic leukemia and high lymphocyte counts after treatment with an anti-CD20 monoclonal antibody (rituximab, IDEC-C2B8). *Blood*. 1999;94(7):2217-2224.
67. Hosokawa M, Kenmotsu H, Koh Y, et al. Size-based isolation of circulating tumor cells in lung cancer patients using a microcavity array system. *PLoS One*. 2013;8(6):e67466.
68. Tatekawa K, Iwata H, Kawaguchi T, et al. Changes in volume of stage I non-small-cell lung cancer during stereotactic body radiotherapy. *Radiat Oncol*. 2014;9:8.

How to cite this article: Nolan RP, Printz MA. Modeling the subcutaneous pharmacokinetics of antibodies co-administered with rHuPH20. *Clin Transl Sci*. 2024;17:e13788. doi:10.1111/cts.13788